Ultrasound Measurement by Laser Doppler Anemometry

P.C.M. Galloway[1], Y. Hardalupas[2] and I. Prassas[2]

[1]DERA Farnborough, UK

[2] Imperial College of Science, Technology and Medicine
Mechanical Engineering Department
Exhibition Road
London SW7 2BX
UK

ABSTRACT

This paper parametrically examines the influence of frequency and amplitude of ultrasound waves in a frequency range of 100-200kHz on the signals produced by a laser Doppler anemometer, as well as the influence of the path length of interaction between laser beams and ultrasound waves. Neutrally-buoyant particles were suspended in water in a cylindrical tank with 130mm diameter and an LDA system, based on a dual Bragg-cell beam splitter and frequency shifter, was used. A high-speed oscilloscope was used to digitise the Doppler signals and frequency analysis was performed on the signals to produce their power spectra. Because of the high frequency of the ultrasound compared with the response time of the particles, the signals were modulated by the variation of the refractive index due to ultrasound field. This finding was also confirmed by use of a stationary glass-fibre scatterer in the probe of the LDA system. The processed signals showed that the measured signal amplitude increased linearly with increasing ultrasound frequency and ultrasound amplitude, for the range of conditions examined here. In addition, a similar relation was found for signal amplitude as a function of the laser beam path length exposed to ultrasound. Theoretical analysis supports the experimental findings. The results suggest that it is feasible to use a laser Doppler-based instrument for the measurement of amplitude of ultrasound sources, provided that certain design guidelines are followed.

1. INTRODUCTION

The possibility of using standard laser Doppler Anemometry (LDA) to measure ultrasound fields has long been recognised. In the past, most efforts were directed towards low frequency ultrasound fields (up to a a few kHz), in which suspended particles were oscillating under the influence of ultrasound waves. In particular, Taylor (1976) used LDA to measure the acoustic particle velocity of smoke in air under the influence of ultrasound of about 10kHz. Taylor (1976) observed that the LDA signals from oscillating particles are frequency-modulated and, therefore, the amplitude of frequency modulation will correspond to the peak velocity of particles and the frequency-to-velocity conversion factor of the LDA system was used to measure the velocity. The technique was later used by the same author for the calibration of microphones (Taylor 1981). Other published work on the measurement of particle oscillation under the influence of sound waves, includes the measurements of standing waves in a water tank by Vignola et al (1991), although the imposed sound frequencies at 1.8 kHz were much lower than those of Taylor (1976, 1981) and the signals were subject to spectral broadening due to particle Brownian motion. The fact that the amplitude of particle oscillation in sound fields depends on their size has been exploited by Strunck et al (1998), who estimated aerosol particle sizes between 0.1 and 20 μm from the oscillation power spectra produced from LDA signals.

Contrary to particle oscillation, local refractive index changes due to ultrasound become important as the frequency increases and dominate when particle response becomes slow. The latter, depending on the type of particles and the medium, is expected to manifest at frequencies higher than a couple of kHz (Crickmore 1997). The phenomenon, which arises due to optical path differences between the two laser beams used in common LDA systems has been theoretically analysed by Jack et al (1998) and their theoretical results were compared with measurements of ultrasound in water of the order of 18kHz (Crickmore et al 1999).

The purpose of the present work was to investigate the effect of ultrasound on LDA signals beyond the range of frequencies examined in previous work (i.e. > 100kHz), in frequencies to which particles remain unresponsive. In addition, the direct effect of the refractive index variations was estimated by use of stationary scatterers to produce LDA signals and variation of the optical path length exposed to the ultrasound waves. In the following sections, a theoretical analysis will be presented to establish the relation between the LDA signals and the parameters varied in the present experiments, followed by the parametric studies of the influence of ultrasound frequency and amplitude, exposed optical path length as well as use of stationary scatterers on the LDA signals.

2. THEORETICAL ANALYSIS

Laser Doppler Anemometry (LDA) in its simplest form requires the use of two laser beams which interact at a given angle and form a probe volume that comprises a fringe pattern due to interference. When a particle crosses the probe volume, the signal produced by photodetectors collecting the scattered light will depict a fluctuation due to the Doppler effect, the frequency of which is linear function of the particle velocity. The application of LDA in the measurement of ultrasound fields requires that the fluid, in which the waves are propagating, is laden with particles that act as laser-light scatterers. Such particles will be oscillating due to the pressure field imposed by the ultrasound source and, therefore, produce a signal due to the Doppler effect. At the same time, the refractive index of the carrier fluid will oscillate due to the pressure field oscillation (e.g. Shutilov 1988) resulting in variations of the optical path length (Crickmore 1997, Jack et al 1998). As a consequence, a phase lag will be introduced between two laser light wavefronts propagating along each beam direction, which depends on the geometrical orientation of the laser beams relative to the direction of propagation of the ultrasound. The consequence of this phase lag is that the interference fringes of the anemometer are oscillating at the frequency of the ultrasound, thus producing a modulation on the signal detected by the photodetectors. It is also known (Crickmore 1997) that for low ultrasound frequencies the signal will mostly originate from particle oscillation (see Taylor 1976 & 1981; Vignola 1991), whilst for high frequencies the refractive index variations dominate (Crickmore 1997). In the following sections we will examine the importance of particle oscillation in the detected signal when

LDA is used in ultrasound fields, as well as the dependence of the signal on the amplitude, the frequency and the laser beam optical path length due the variation of the refractive index of the carrier fluid.

2.1 Particle response to ultrasound fields

Particle ability to follow the fluid velocity due to the ultrasound wave depends on their physical properties, as well as that of the carrier medium and is an inverse function of the frequency of the ultrasound waves. As the ultrasound frequency increases the amplitude of particle oscillation due to ultrasound decreases and the particle motion lags behind that of the ultrasound. Analytically, the ratio of the amplitude of the particle oscillation over that of the ultrasound reads (Hjelmfeld and Mockros 1966):

$$h = \sqrt{(1+ f_1)^2 + f_2^2} \tag{1}$$

where

$$f_1 = \frac{(1-s)/(s+\frac{1}{2})}{\left(\frac{18N_s^2}{s+\frac{1}{2}}\right)^2 + 1} \tag{2}$$

and

$$f_2 = \frac{\frac{18N_s^2}{\left(s+\frac{1}{2}\right)^2}(1-s)}{\left(\frac{18N_s^2}{s+\frac{1}{2}}\right)^2 + 1} \tag{3}$$

In equations (2) and (3), $s = r_p / r_f$ is the ratio of particle and the fluid velocities and:

$$N_s = \sqrt{\frac{n}{w d^2}} \tag{4}$$

,

is the particle Stokes number, where n is the fluid kinematic viscosity, w is the ultrasound cyclic frequency and d is the particle diameter. Similarly, the phase difference between the ultrasound and the particle oscillations is:

$$b = \tan^{-1}\left(\frac{f_2}{1+ f_1}\right) \tag{5}$$

It is quite obvious according to this analysis that if particle density equals that of the carrier fluid (i.e. s=1) there will be no phase lag and the amplitudes of both oscillations will be equal. Practically, one has to select particles with density as close to that of the medium as possible, not only to optimise the response, but also to ensure that particles do not drift due to the influence of gravity and eventually sediment in the test vessel.

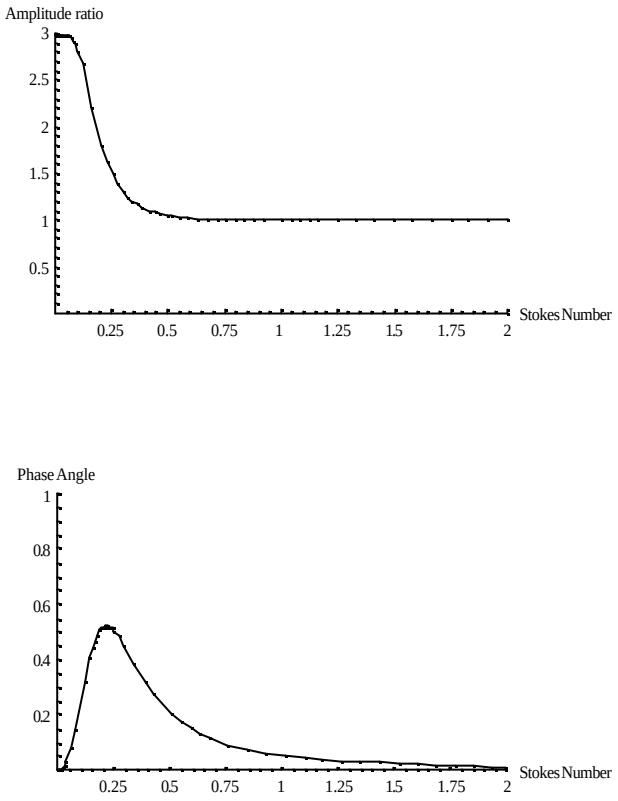

Fig 1 (a) Amplitude ratio of the particle oscillation and the ultrasound source (top) and (b) phase difference between the two oscillations(bottom) as a function of the particle Stokes number

It is also obvious from equation (4) that as the frequency of the ultrasound increases the Stokes number N_s decreases and therefore both parameters f_1 and f_2 increase. As a consequence, the phase lag deviates from zero and the amplitude ratio from unity. If we use the physical properties of the particles used in the current experimental campaign (see section 3.4), the results are summarised in figures 1a and 1b, which present the amplitude ratio of the two oscillations along with the phase lag between them.

From the graphs, one can estimate that the particles under consideration will faithfully follow oscillations of up to about 4kHz, which is two orders of magnitude smaller than the frequencies considered in this work. Note that due to assumptions in the derivation of the equations for the particle response which include neglecting the Basset history term, it is likely that for high frequencies particle response will be *worse* than that predicted by the theory. Also, problems may be expected even for particles with the same density as the fluid, due to the large size of the 'seeding' particles relative to the expected displacements (of the order of 100 nm) due to ultrasound excitation. The non-instantaneous response of particles to the excitation has been exploited by Strunck et al (1998) to derive the size of the particles.

2.2 Refractive index fluctuation due to ultrasound

Following Shutilov (1988), the velocity potential of a monochromatic plane wave, with infinitesimal amplitude, from an ultrasound source that oscillates harmonically with (cyclic) frequency w is described from:

$$j(x) = j_{\max} \cdot \sin(wt - kx) \tag{6}$$

Where $j_{\max}$ is the amplitude of the velocity potential, k is the wave number of the ultrasound and x is the distance travelled by the wave from its source. The velocity of the fluid particles can be derived from differentiation of the velocity potential. Consequently, the amplitude of the fluid particle velocity is:

$$v_{\max} = k j_{\max} \tag{7}$$

The amplitude of the pressure field can also be deduced and is:

$$p_{\max} = r_0 c_0 v_{\max} \tag{8}$$

where r_0 is the density of the undisturbed fluid and c_0 is the wave propagation velocity in the undisturbed fluid. Accordingly, the fluid density will fluctuate in phase with the pressure field with amplitude:

$$r_{\max} = \frac{p_{\max}}{c_0^2} \tag{9}$$

The result of the density fluctuations is that the refractive index of the fluid n fluctuates, with amplitude:

$$n_{\max} = \frac{r_{\max}}{r_0} N_0 \tag{10}$$

where

$$N_0 = \frac{\left(n_0^2 - 1\right)\left(n_0^2 + 2\right)}{6n_0} \tag{11}$$

appears due to the functional relationship between refractive index and density, known as the Lorenz-Lorenz equation.

Another useful relationship can be derived by integrating the instantaneous fluid particle velocity to yield the fluid particle displacement. The amplitude of the displacement is known as amplitude of oscillations in an ultrasonic wave A is:

$$A = \frac{v_{\max}}{w} \tag{12}$$

Combining equations (8)-(12) one yields the relation between refractive index amplitude and ultrasound frequency and amplitude:

$$n_{\max} = \frac{N_0}{c_0} A w \tag{13}$$

which can also be written as $N_0 A k$, where $k = w / c_0$ the wave number of the wave. This equation shows that the refractive index is linearly dependent on the amplitude of the ultrasound oscillations and the ultrasound wave frequency.

2.3 Signal modulation due to refractive index oscillation

In the following paragraphs the theory of the signal modulation due to refractive in dex oscillation is presented. A particle is assumed to be held stationary in the LDA probe volume and is not oscillating under the influence of the ultrasound and that a frequency shift has been introduced and the fringes are moving at constant speed relative to the stationary scatterer. This is equivalent to saying that the fringes are stationary and the particle is moving relative to them with velocity that corresponds to the frequency shift. The photodetector signal will have constant amplitude and frequency. If an ultrasound field is imposed to the fluid, the refractive index variations will result in oscillatory motion of the fringes at the frequency of the ultrasound, which is independent of the imposed frequency shift. In addition, the amplitude of fringe oscillation is directly proportional to the refractive index fluctuations which according to the analysis of section 2.2 is linearly dependent on the amplitude of the ultrasound waves.

According to the description of the previous paragraph, the ultrasound acts as a FM modulator of the signal originating from the frequency shift (carrier signal). An FM modulator produces a maximum frequency modulation Δw that corresponds to maximum modulating amplitude (Pratt and Bostian 1986). In the current analysis, the maximum modulating amplitude is the amplitude of oscillation of the ultrasound. In our case, where the modulator is a monochromatic plane ultrasound wave at frequency $w_{\mathrm{mod}} = 2p\ f_{\mathrm{mod}}$ and the carrier frequency is the imposed frequency shift $w_{sh} = 2p\ f_{sh}$, the FM-modulated signal (i.e. the signal detected by the LDA photodetector) is described as:

$$u(t) = A_{sh} \cos\left[w_{sh} t + \left(\frac{\Delta w}{w_{\mathrm{mod}}} \right) \sin(w_{\mathrm{mod}} t) \right] \tag{14}$$

where

$$m = \frac{\Delta w}{w_{\mathrm{mod}}} \tag{15}$$

is the modulation index m and takes a value for Δw that corresponds to the amplitude of the ultrasound oscillation. In other words, the amplitude of the ultrasound has been mapped into a frequency described by the modulation index. A typical power spectrum of a FM-modulated signal looks like that of figure 2, although the number of distinctive frequency lines appearing in the spectrum depend on the modulating frequency (the ultrasound frequency), the carrier frequency (the frequency shift) and the amplitude of ultrasound.

Analytically a FM signal can be written as a series of Bessel functions of the first kind that depend on the modulation index. Each peak in the spectrum corresponds to a Bessel function of order n, with the carrier peak (the central peak) corresponding to order 0 and every other satellite peak to an increasing order from the carrier. Practically the ratio of the amplitudes between two peaks is equal to the ratio of the Bessel functions of the appropriate order. In other words:

$$\frac{A_1}{A_0} = \frac{J_1(m)}{J_0(m)} \tag{16}$$

from which equation one can estimate the modulation index for the given signal. Recall from equation (15) and the theory of FM signals that the modulation index is proportional to the amplitude of the modulation

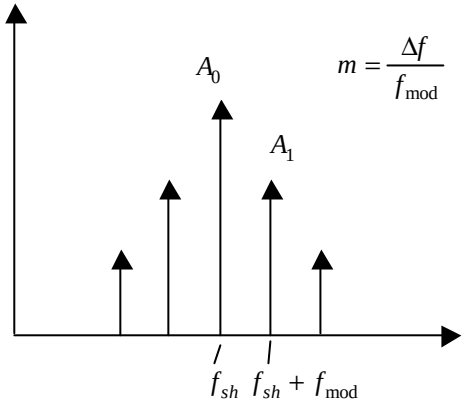

Fig. 2 Schematic of a power spectrum of a frequency-modulated signal

signal, i.e. the ultrasound amplitude, and therefore the modulation index calculated from the power spectrum is a measure of the ultrasound amplitude.

It should be noted that the number of peaks appearing in the spectrum of such a signal, which is a function of the modulation index (only three peaks for m<<1, more as m increases beyond unity) depends on the frequency shift (carrier frequency) used in the measurements. If the frequency shift is large relative to the modulating frequency, m is likely to remain below unity and, hence, only three peaks will appear. The higher the frequency shift, the higher the available bandwidth in FM modulation and, hence, the less the energy that is contained in peaks beyond the first satellite.

3. EXPERIMENTAL ARRANGEMENT, INSTRUMENTATION & CONDITIONS

3.1 Optical Arrangement

The LDV system comprised a 30 mW He-Ne laser (Melles-Griot) operating at 632.8 nm, a beam splitter and double Bragg-cell-based optical shifter which, for the purposes of the present experiments, provided stable frequency shift of 1 and 2 MHz by driving the Bragg cells around their nominal operating frequency of 80MHz. The two optically-shifted beams were focused by a f/250 singlet to form the probe volume. The beam intersection angle was 7.522° and the spacing of the interference fringes in the probe volume was 4.823 μm. Light scattered from the LDV probe volume was collected by an f/300 commercially-available unit (Dantec, model X0341) and converted to current by a Photomultiplier tube (Burle, model 4526). The high-voltage power supply to the photomultiplier tube varied depending on the location of the probe volume and the type of scatterer used between 1.2 and 1.4 kV. The optical arrangement along with the flow configuration is shown in figure 3.

3.2 Pressure Transducer & Driving Electronics

An ultrasound pressure transducer (National Physical Laboratory, UK, part number W002, Met-Opt. Piston) was used for the experiments, driven by an RF power amplifier (ENI Inc, model 240L) operated at 10-200 W/50Ω output. The power amplifier was fed with sinusoidal signals of 160-570 MV at frequency equal to the desired frequency of the pressure waves, which varied between 100 and 200 kHz. The

sinusoidal signals were provided by a function generator (Wavetek, model 145). The ultrasound source calibration curve was not available at the time of measurements. This however, does not harm the generality of the results.

3.3 Signal Digitisation

The output signals of the photomultiplier were directed into a digital oscilloscope (LeCroy, model 9350AM) and were digitised at 5MHz sampling rate. 500,000 samples were collected for each Doppler signal, which corresponded to the maximum number of samples that can be stored in the memory of the oscilloscope. The samples were stored on floppy diskettes and were subsequently processed by the FFT module of the oscilloscope, using a *Blackman-Harris* window function. This function provided (Anon. 1995) the minimum power leakage of all common FFT window functions, albeit at the expense of frequency resolution. The latter was not an issue in the present experiments, since the driving frequencies were known *a priori*. In order to reduce the influence of noise and to improve the accuracy of the measured signal power at the desired frequencies of the power spectrum, average spectra over 5 sweeps were produced and each individual spectrum was generated from signals at sampling rates mentioned earlier.

3.4 Flow Configuration

A cylindrical water tank made of Perspex with 130 mm diameter and 440 mm height was used for the measurements (figure 3). The tank was filled with de-ionised water (Fisher Scientific Corp., product W/0100/25) chosen to contain a minimum number of impurities which would scatter laser light. The pressure transducer was mounted near the top of the tank in such a way that the axis of propagation of the acoustic waves was aligned with the centreline of the tank. The source of waves was about 150 mm above the LDV probe volume. The tank bed was covered with special sound absorbing material to ensure that no acoustic waves were reflected back and interfered with the incoming waves. For the cases where particles were suspended in the flow, plastic spheres of 6 µm mean diameter and 1.07 kg/m^3 density were used (Sekisui, Japan, type SBX). The particles were selected to be as small and as responsive as possible, whilst having a density close to that of de-ionised water so that no particle sedimentation occurred during the course of the measurements.

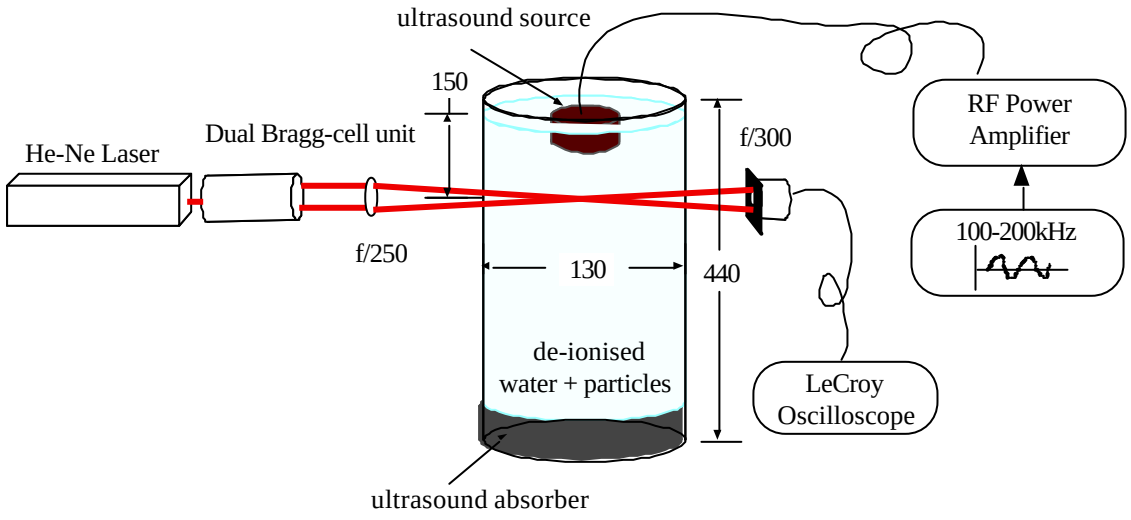

Fig 3. Experimental arrangement

For the experiments with stationary scatterers, a 20 mm-long glass fibre of 150 μm diameter was used and was mounted across the branches of a V-shaped post. The fibre was then placed in the centre of the LDV probe volume by ensuring that a continuous LDV signal was produced by its presence.

3.5 Experimental Conditions

Table 1 describes the experimental conditions of the experiment. Cases IA-IIIC correspond to experiments with suspended particles, whilst cases ID-IIID correspond to the experiments using the stationary glass fibre. For the latter experiment, an oscillating frequency of 200 kHz was used, similar to the experiments corresponding to cases IC-IIIC.

Voltage [mV](Power [W])	100 kHz	150 kHz	200 kHz	Fibre
160 (10)	IA	IB	IC	ID
370 (75)	IIA	IIB	IIC	IID
580 (200)	IIIA	IIIB	IIIC	IIID

Table 1 Experimental conditions

4. RESULTS

Figure 4 presents sample snapshots from the LeCroy oscilloscope for two of the cases presented in table 1. The snapshots show the original signal as well as the power spectra from which the amplitude of the oscillation was estimated. In those figures peaks are present at 1MHz as well as at frequencies 1±F MHz, where F was the frequency of the acoustic waves, in the range of 0.1-0.2 MHz. Note that the top signal in each window is the original Doppler, the middle is the corresponding power spectrum and the bottom is the average spectrum of 5 spectra from consecutive signals. Other peaks can be also observed, at frequencies unrelated to those of the acoustic waves (although in some cases, peaks correspond to harmonics of the basic oscillation frequency). In some cases peaks were detected at 0.5 MHz, which was half the frequency of the imposed frequency shift; however the reason for their occurrence is not currently understood. It is unlikely, though, that those peaks influence the accuracy of the present measurements, since the frequency

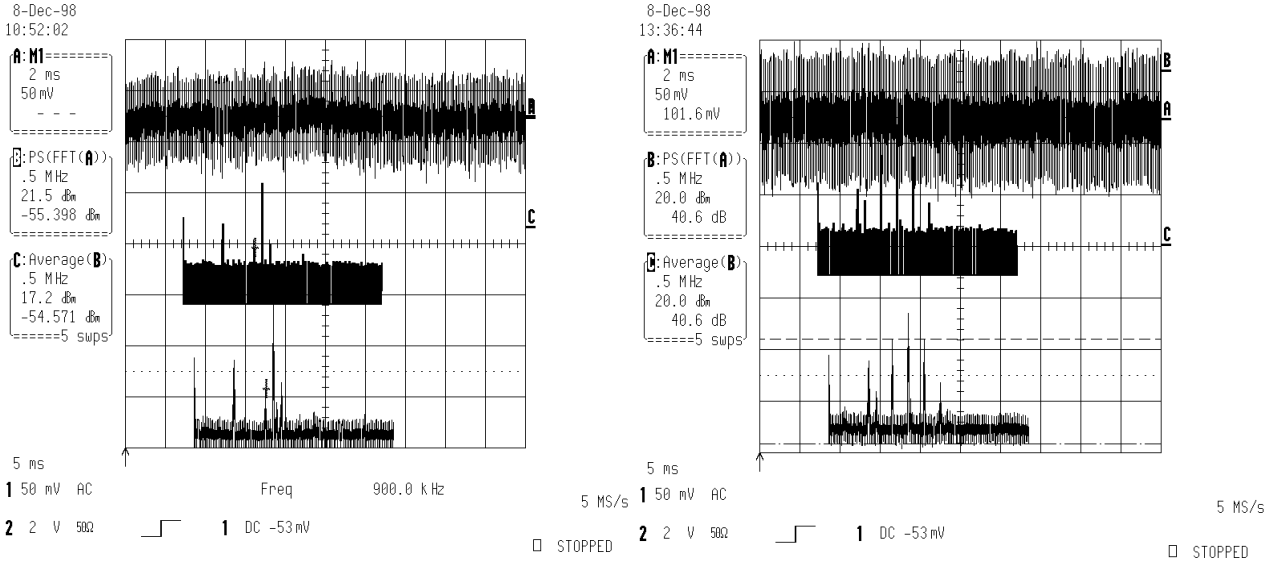

Fig. 4 Sample signal power spectra corresponding to cases IA (left) and IIIC (right)

of the imposed acoustic waves was known and, therefore, amplitude measurements were taken at well-defined conditions.

The peaks due to the ultrasound waves were symmetrically located around the central peak of 1MHz of the frequency shift to within 10 kHz precision. It is likely that the 1% deviation between the expected frequency (1±F) and the measured frequency was due to the window function used in the construction of the power spectrum and due to frequency drifting of the function generator. It should be noted, however, that the repeatability of the frequency at which the peaks occurred between successive measurements was perfect for a given condition. In order to ensure that there was no influence on the measurements from the LDV frequency shift a set of measurements at 2MHz frequency shift were made, but no differences in the measurements obtained at 1MHz and 2MHz frequency shifts were observed.

The power of the 1 MHz peak as well as its satellite peaks due to the acoustic waves were measured directly on the screen of the oscilloscope (in dB) and the frequency modulation index was then calculated from equation (16). The measurements were first performed as a function of the frequency of the ultrasound as well as the amplitude of the signal driving the ultrasound source and the results are respectively shown in figures 5 and 6. It is obvious in both cases that the modulation index (and, as a consequence, of the amplitude of the ultrasound) is a linear function of the frequency and the amplitude of the ultrasound source for the parameter ranges used here, as expected from theory (equation 13).

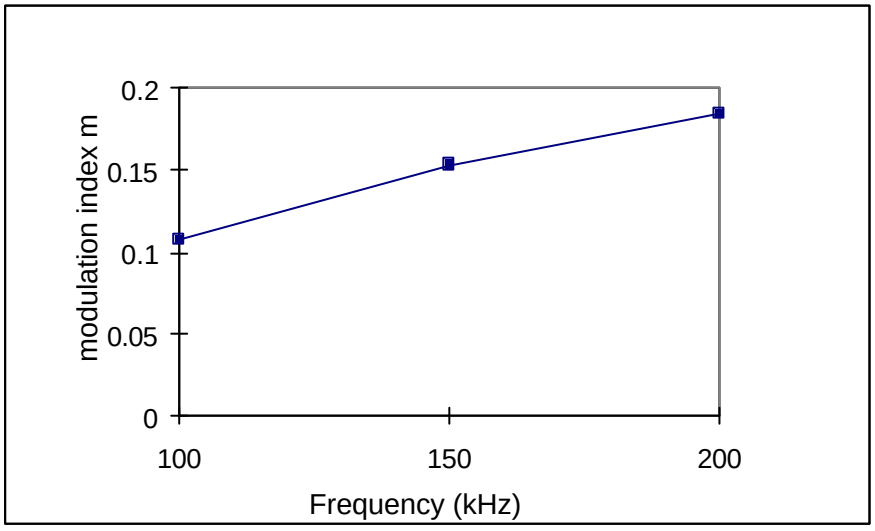

Fig. 5 Doppler signal modulation index as a function of the frequency of the ultrasound source

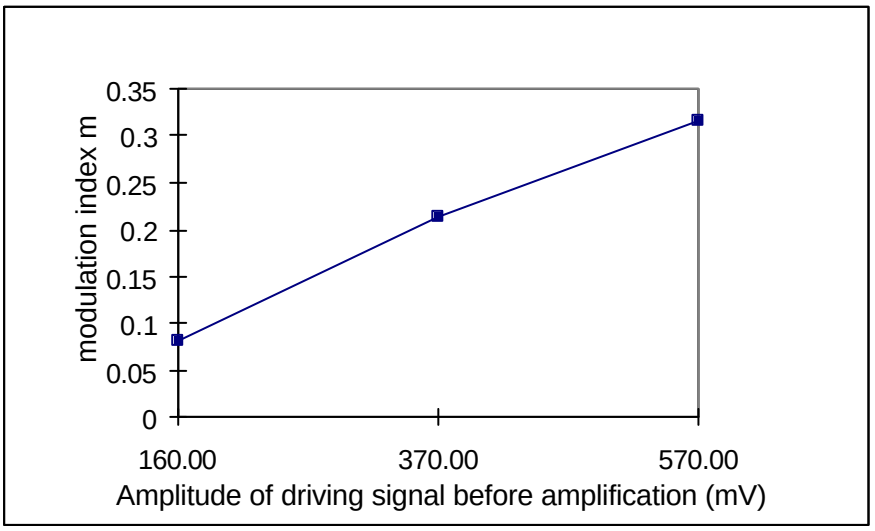

Fig. 6 Doppler signal modulation index as a function of the amplitude of the ultrasound source

Because of the magnitude of the frequency of the imposed ultrasound waves in the present experiments and the analysis of section 2.1 it was deemed unlikely that the suspended particles oscillated under wave influence, resulting in the characteristic lines in the power spectrum. For this reason, two further experiments were conducted, results of which are depicted in figures 7 and 8. Figure 7 shows the results from traversing the probe volume of the LDV system along the axis of propagation of the laser beams

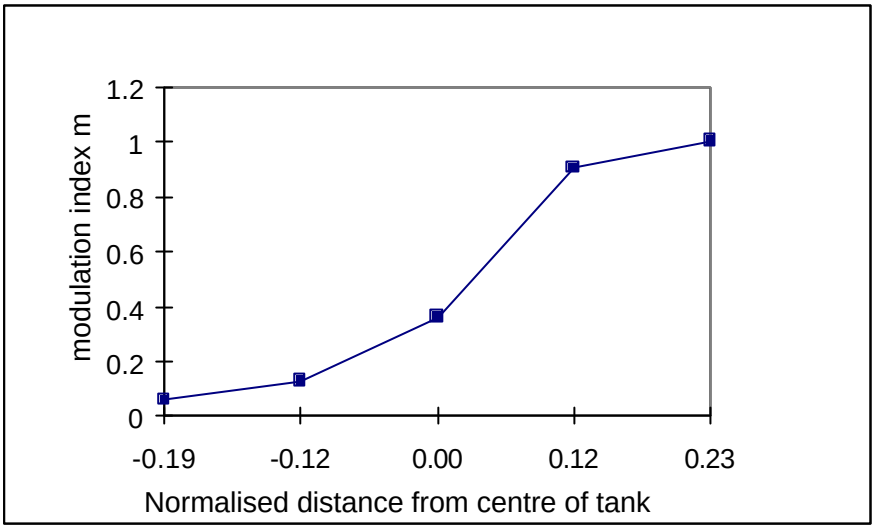

Fig. 7 Doppler signal modulation index as a function of the normalised distance of the LDA probe volume from the centreline of the tank

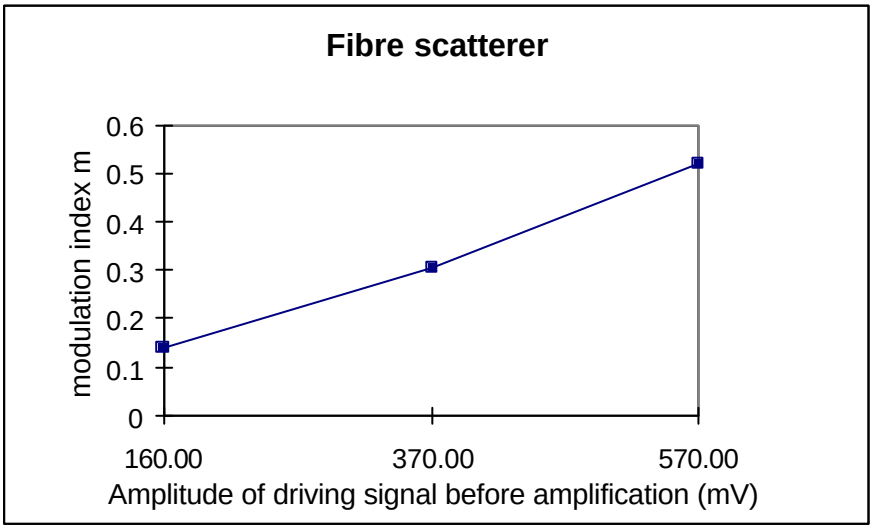

Fig. 8 Doppler signal modulation index as a function of the amplitude of the ultrasound source in the case of a stationary fibre scatterer.

(normal to the propagation of the ultrasound waves) for conditions corresponding to case IIC. Had the source of the characteristic lines in the spectrum been particle oscillation, the power of the spectrum at the characteristic frequencies should remain constant, since thorough stirring of the water in the tank ensured that the particle density and size distribution across a cross-section of the tank was constant. In addition, there is no particular reason why particles should follow the ultrasound waves differently depending on the distance from the centreline of the tank. However, the results show that the modulation index is clearly a monotonic function of the location and is, in fact, increasing with increasing laser beam optical path in the

tank. In the central region of the tank the modulation index is approximately a linear function of the optical path whilst away from centreline its value reaches a plateau. The latter for positive normalised distances is probably due to distortion of the ultrasound waves away from the centreline of the source (the sound source was cylindrical with about 65 mm diameter), whilst for negative ones due to small optical path length in the ultrasound field, which results in amplitude of the modulated signal with low signal to noise ratio.

This suggests that the reason was the variation of the refractive index of the fluid along the propagation of the beams. It is expected that the modulation index is a linear function of the optical path length provided that the waves remain infinitely flat (Crickmore 1997) Note that experiments were also conducted with the normal to the plane of the laser beams aligned with the propagation of the ultrasound waves and the probe volume at the centreline of the tank, for conditions corresponding to case IIC. The peaks corresponding to the acoustical oscillations were just above the noise level. This is not surprising, particularly if we take the theoretical results of Crickmore et al (1999) into account, since the plane of the beams is parallel to the ultrasound waves and thus, any optical variations will be equal on both beams and hence cancel out.

In order to confirm that we observed refractive index fluctuations in the present experiments the water in the tank was replaced with fresh clean de-ionised water and a rigid fibre scatterer was placed in the LDV probe volume. Monitoring of the LDV signal in the absence of the waves indicated that the signal amplitude was almost constant, as one would expect with stationary scatterer. Figure 8 shows the variation of the modulation index as a function of the amplitude of the driving signal. The influence of the ultrasound waves (see table 1 for conditions) was similar to the case of the suspended particles, suggesting that in both cases it was indeed the effect of the ultrasound on the refractive index, rather than physical oscillation, which was after all unlikely due to the physical dimensions and the mounting of the fibre scatterer.

5. DISCUSSION

With the exception of the recent results by Crickmore et al (1999),who nevertheless used ultrasound of one order of magnitude lower frequency than ours, the current paper provided evidence that LDA can be used to characterise ultrasound sources. The advantage of the present setup over that of Crickmore et al (1999) is that a continuous laser source was used, which is much simpler to align and use than a pulsed source. Because the frequency modulation index is a linear function of the amplitude of the ultrasound, reciprocal calibration with a reference hydrophone is possible. Moreover, provided that the frequency shift is high enough compared with the ultrasound frequency (e.g. using Carson's rule, $f_{sh} = 2\, f_{\mathrm{mod}}\,(m+1) \cong 4\, f_{\mathrm{mod}}$) the LDA instrument should be able to operate at frequencies at which mechanical damping may be significant. An instrument for hydrophone calibration is more probable that will have to be inserted in a water tank. It is an advantage to have an optical arrangement with a particle scatterer always in the probe volume and collect light at 180° (i.e. backscatter) relative to the direction of the beams.

6 CONCLUSIONS

A standard laser Doppler anemometer was used to measure ultrasound fields at frequencies of 100-200kHz as a function of the ultrasound frequency, its amplitude and the optical path length of interaction. The ultrasound source was immersed in a tank filled with de-ionised water, whilst neutrally-buoyant particles were suspended in the fluid to generate the signals. The Doppler signals were digitised and analysed in the frequency spectrum. The frequency modulation index, which is proportional to the amplitude of the ultrasound was calculated in each case. The results, which are supported by theoretical considerations, show that:

1. The modulation index is increasing proportionally with the amplitude and the frequency of the ultrasound.
2. With the exception of near wall regions, the modulation index increases linearly with the laser beam optical path length in the ultrasound field.
3. The only phenomenon measured by the current instrument was refractive index fluctuation and not particle oscillation, as confirmed by similar results produced when a fixed optical scatterer was used in the place of suspended particles.

The current results suggest that LDA, in conjunction with conventional techniques at low frequencies, can be used to calibrate ultrasound sources, particularly at high frequencies where refractive index fluctuations dominate. An optical head was suggested for ultrasound measurements, which will operate in backscatter mode and observe the scattered light form a stationary scatterer always present in the probe volume.

REFERENCES

Anon. (1995) LeCroy Digital Oscilloscopes 9350/54 Series: Operator's manual.

Crickmore, R. I. (1997). The laser doppler hydrophone: theoretical and experimental studies. 7th Int. Conf. On Laser Anemometry, Advances and Applications, Karlsruhe, pp. 35-42.

Crickmore, R. I., Jack, S. H., Hahn, D. B. and Greated, C. A. (1999). Laser Doppler anemometry and the acousto-optic effect. Optics and Laser Technology 31, 85-94

Hjelmfelt Jr, A. T. and Mockros, L. F. (1966). Motion of discrete particles in a turbulent fluid. Appl. Sci. Res. 16, 149-161.

Jack, S. H., Hahn, D. B. and Greated, C. A (1998). Influence of the acousto-optic effect on laser Doppler anemometry signals. Review of Scientific Intruments 69(12), 4074-4081.

Pratt, T. and Bostian, C. (1986). Satellite communications. John Wiley and Sons, New York.

Shutilov, V. A. (1988). Fundamental physics of ultrasound. Gordon and Breach Publishers, London.

Strunck V., Mueller, H., Grosche, G. and Dopheide, D. (1998). Aerosol size measurement using a laser Doppler probe and acoustic excitation of the fluid flow. 9th International Symposium of Application of laser Techniques to Fluid Mechanics, paper 18.3.1.

Taylor, K. J. (1976). Absolute measurement of acoustic particle velocity. J. Acoust. Soc. Am. 59(3), 691-694.

Taylor, K. J. (1981). Absolute calibration of microphones by a laser-Doppler technique. J. Acoust. Soc. Am. 70(4), 939-945.

Vignola, J. F., Berthelot, Y. H. and Jarzynski, J. (1991). Laser detection of sound. J. Acoust. Soc. Am. 90(3), 1725-1286.